Slope Stability Analysis Using Finite Element Techniques

Colby C. Swan, Assoc. Professor
Young−Kyo Seo, Post−Doctoral Research Assoc.

Civil & Environmental Engineering
Center for Computer−Aided Design
The University of Iowa
Iowa City, Iowa USA

13th Iowa ASCE Geotech. Conf.
12 March 1999
Williamsburg, Iowa

LIMIT STATE ANALYSIS OF EARTHEN SLOPES USING DUAL CONTINUUM/FEM APPROACHES

A. Review of Classical Methods

B. Proposed Slope Stability Analysis Methods

* Gravity Increase Method
* Strength Reduction Method

C. Comparison of the Methods for Total Stress Analysis

D. Application to Problems with Seepage

E. Assessment of Continuum/FEM Approaches to SSA

A. Review of Common Classical Methods

* Infinite Slope Analysis
* Mass Methods (Culmann's method; Fellenius−Taylor method)
* Methods of Slices (Bishop's simplified method, Ordinary method of slices,...)

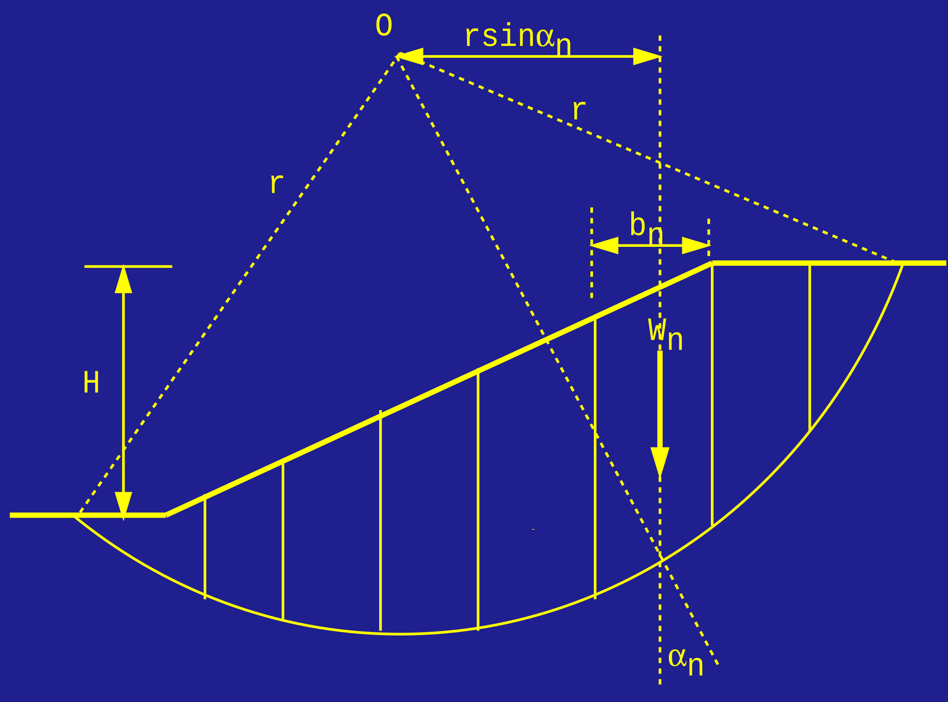

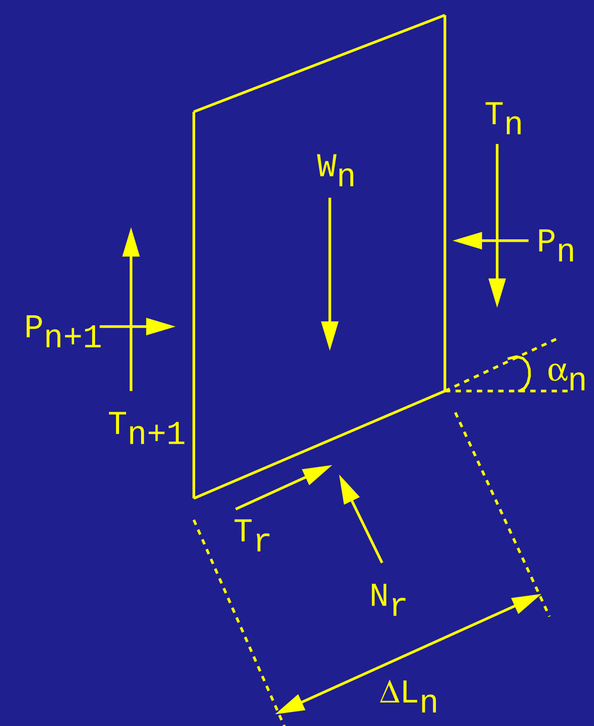

* Factor of Safety:

$$FS = \frac{M_R}{M_D}$$

where M_R= The moment of ultimate resisting forces

M_D= The moment of driving forces

* Perceived shortcomings in classical methods:

1) Analysis of stresses within the soil mass is approximate.

   a) Using statics approximations for continuum system.
   b) Interslice forces?

2) Typically restricted to Mohr−Coulomb soil models

   * Other, more realistic soil models are presently available. (Critical state models; cap models; softening effects; etc)

3) Transient effects associated with pore pressure diffusion are difficult to incorporate.

* Research question:
  Can continuum/FEM methods be applied to improve state of the art in SSA?

B. Two Continuum/FEM Slope Stability Analysis Techniques

<u>Gravity Increase Method</u>

* Increase **g** until the slope becomes unstable and equilibrium solutions no longer exist. (W.F. Chen)

* $g(t)=g_{base} * f(t)$ where g_{true} is actual gravitational acceleration.

$$* \ (F.S)_{gi} = \frac{g_{limit}}{g_{true}}$$

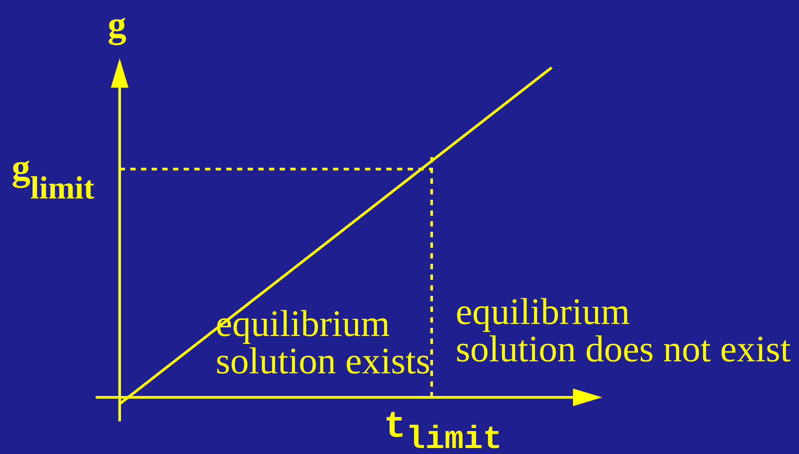

<u>Strength Reduction Method</u>

* Decrease the strength parameters of the slope until slope becomes unstable and equilibrium solutions no longer exist. (D.V. Griffiths, and O.C. Zeinkiewicz)

* $Y(t)=Y_{base} * f(t)$ where Y_{base} are actual strength parameters

$$* \ (F.S)_{sr} = \frac{Y_{base}}{Y(t_{limit})} = \frac{1}{f(t_{limit})}$$

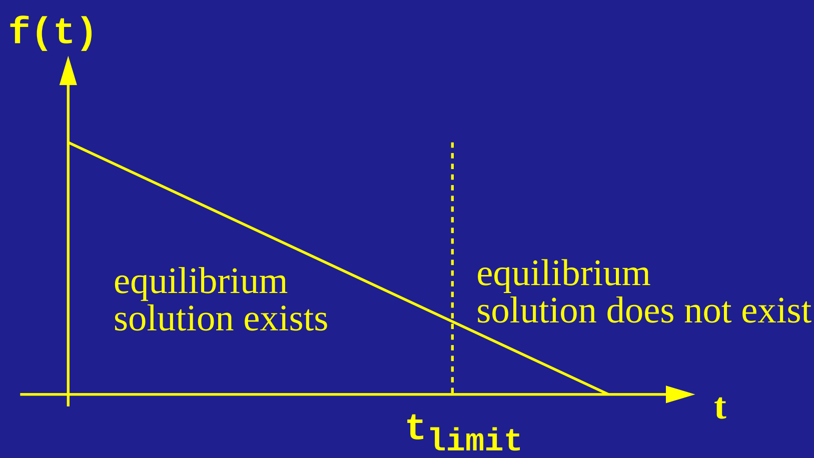

Fit of Drucker−Prager Yield Surface

with Sand Data of Desai and Sture.

$$* \quad f(\sigma) = \|s\| - \{ \alpha + \lambda (1 - \exp [\beta I_1]\} \leq 0$$

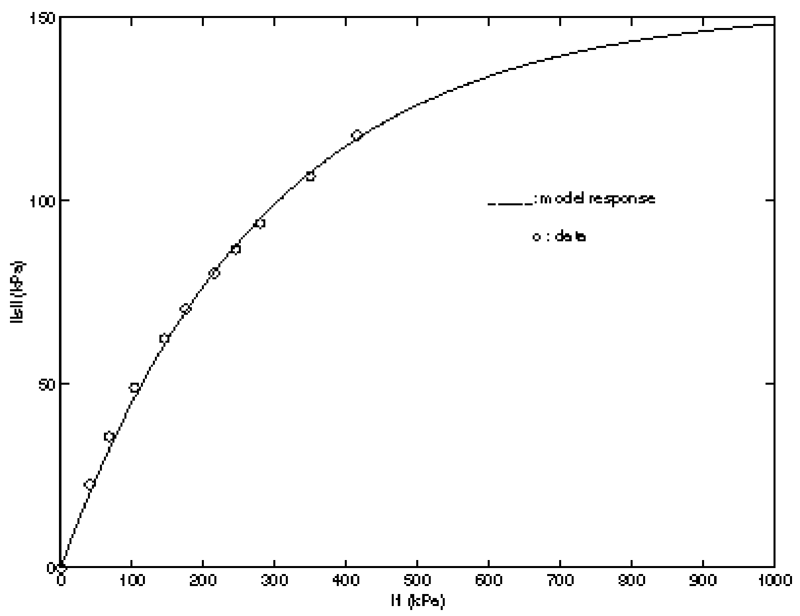

λ = 1.53 kPa, β = 3.48d−6 Pa^{-1}, α=0

Application of Loads to Soil Mass (For gravity method)

<u>Note:</u> For purely frictional soils (non−cohesive), shear strength comes entirely from effective confining stresses.

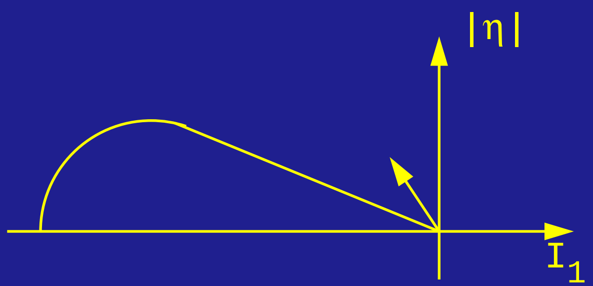

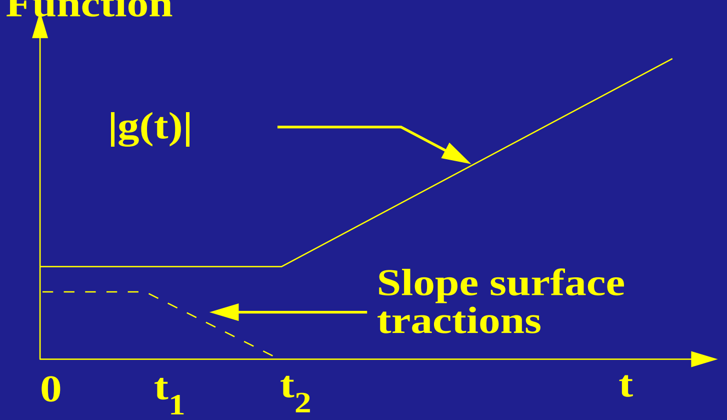

a)Load−time functions for gravity and surface tractions.

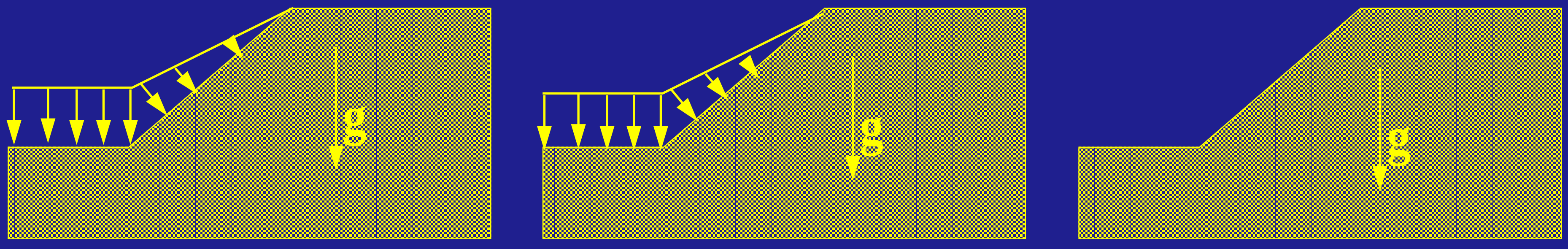

b) $0<t<t_1$ c) $t_1<t<t_2$ d) $t>t_2$

C. Comparative Results (Total Stress Analysis)

1) Non−frictional Soil (α = 141kPa)

$(FS)_{gi}$=3.03, $(FS)_{sr}$=3.04 ; Fellenius−Taylor Method ; FS=3.17

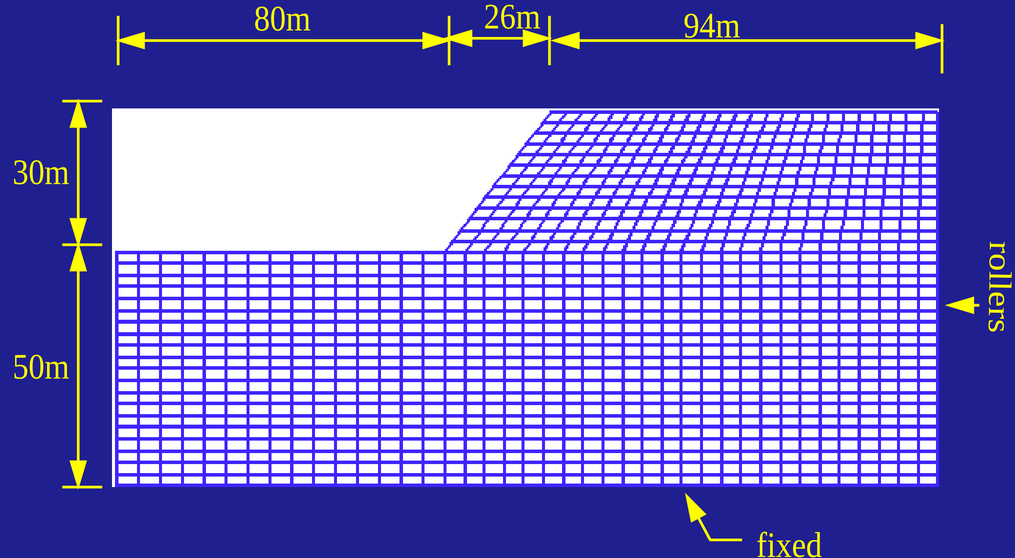

a) Undeformed slope.

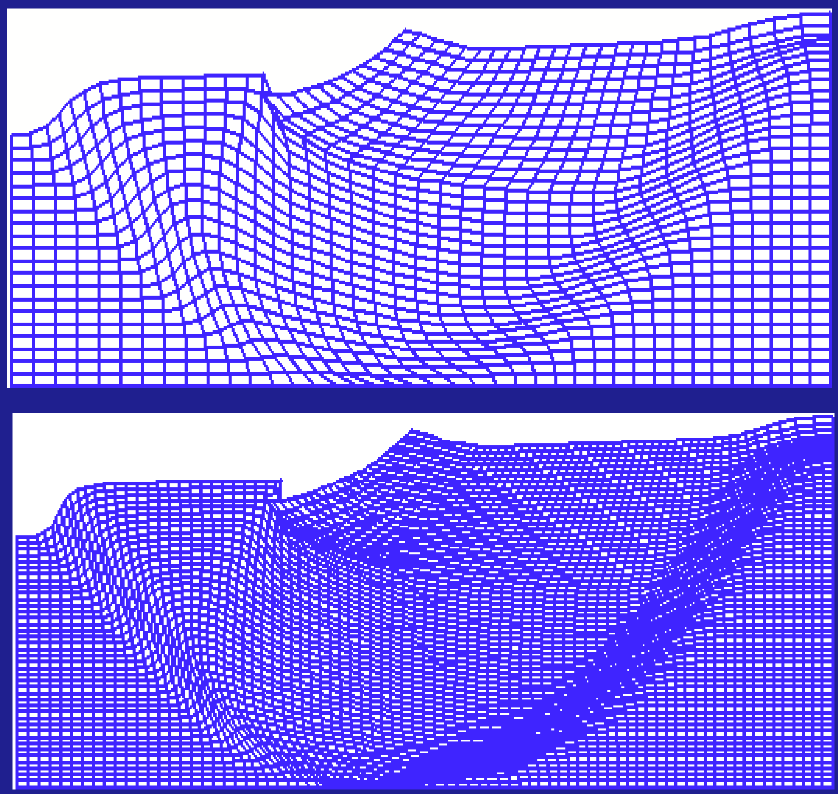

b) Deformed slope at limit state.

2) Frictional Soil: Slope angle 20º (λ = 1.53 kPa, β = 3.48d−6 Pa^{-1}, α=0)

Strength Reduction Method | **Gravity Increase Method**

H=6m

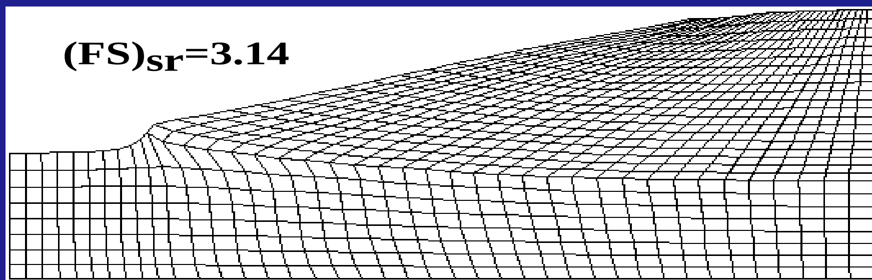

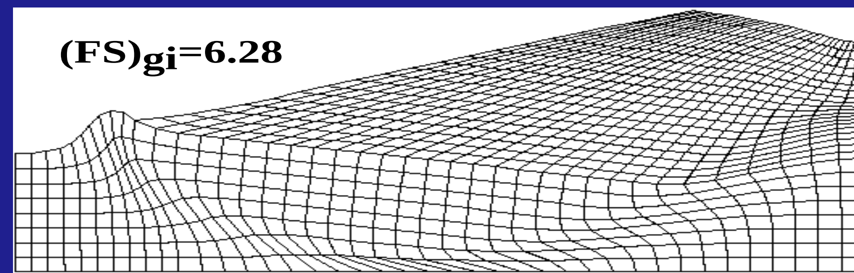

H=12m

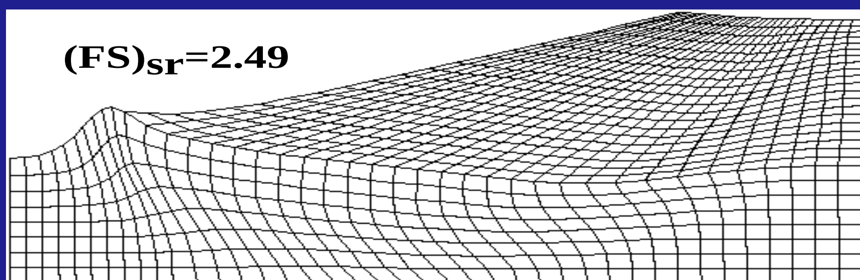

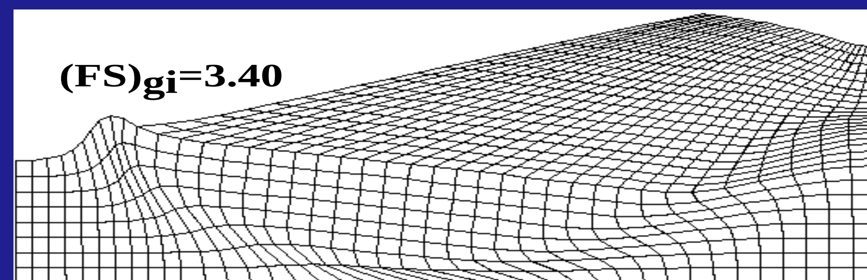

H=30m

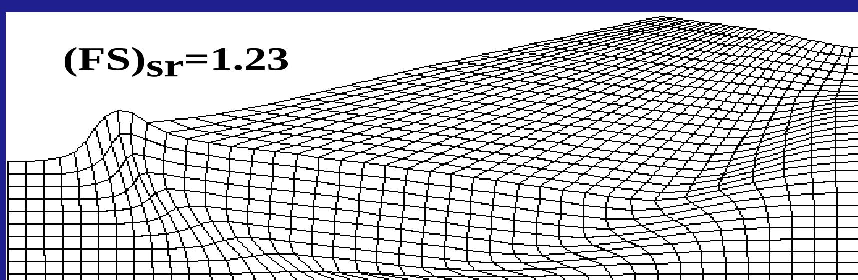

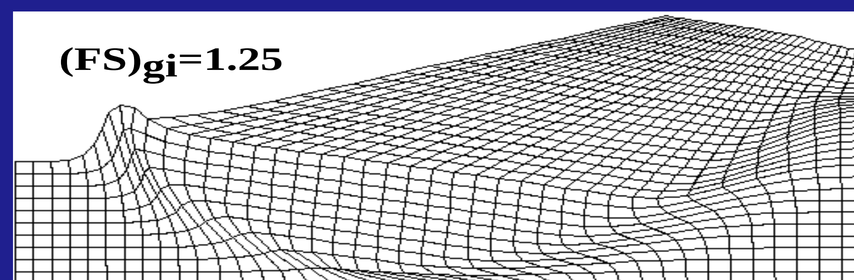

H=60m

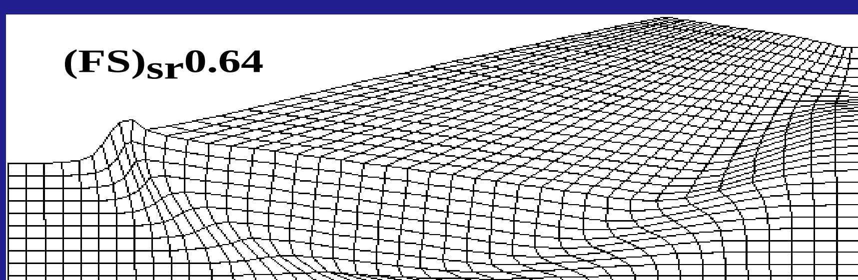

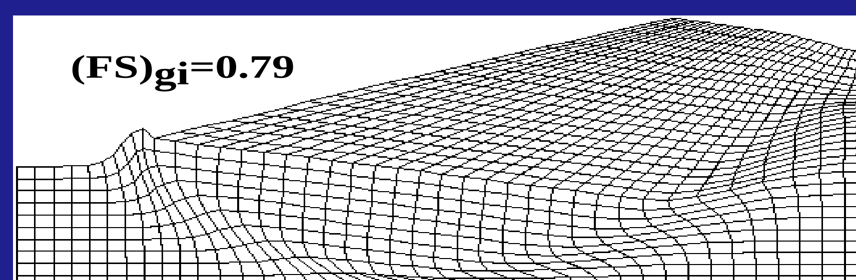

3) Heterogeneous Soil: Slope angle 30^{o}

Clay: α = 141kPa(dark region)

Sand: λ = 1.53 kPa, $\beta = 3.48d{-}6\ Pa^{-1}$, α=0

<u>Strength Reduction Method</u> <u>Gravity Increase Method</u>

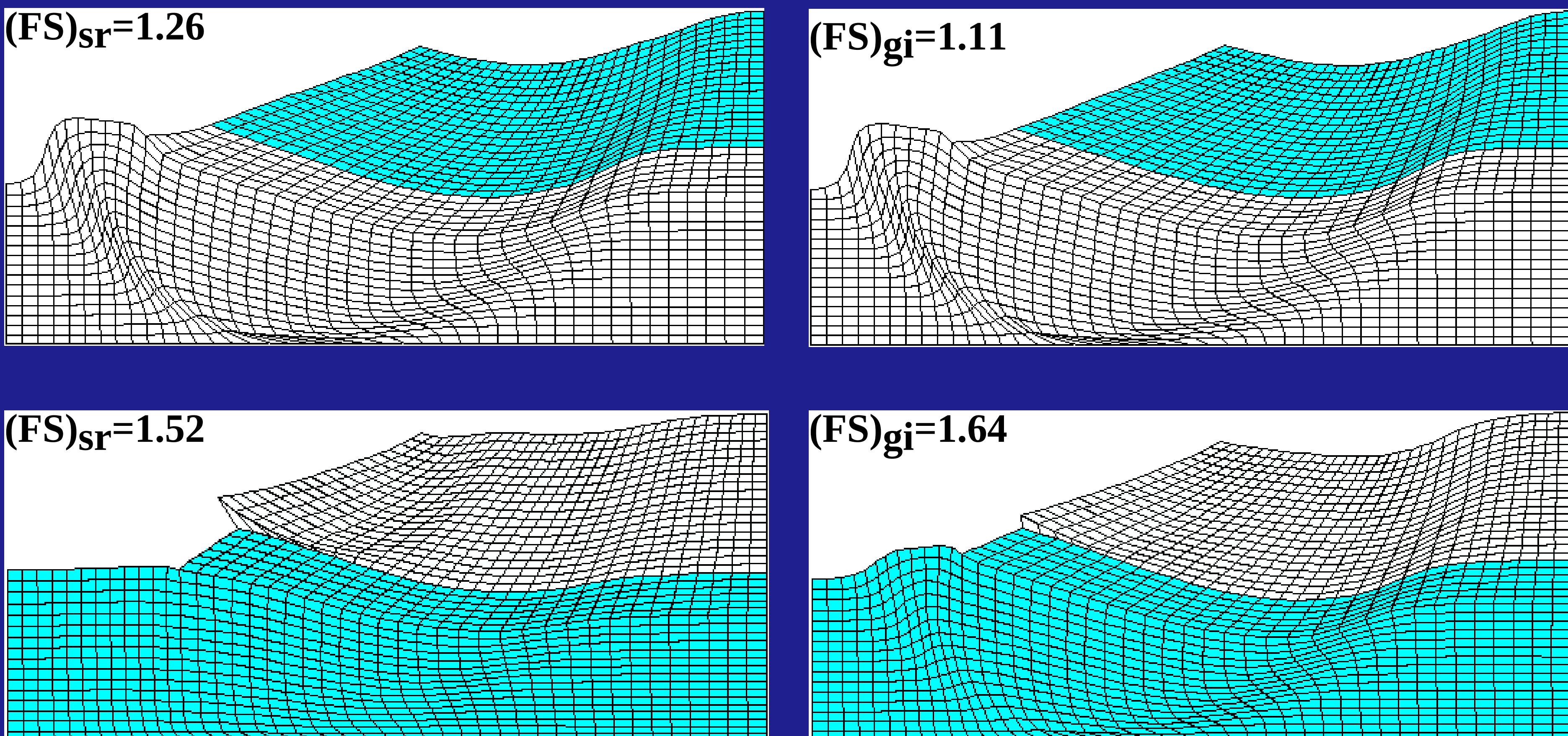

Steep Slope with tension crack 1   Clay:α = 141kPa

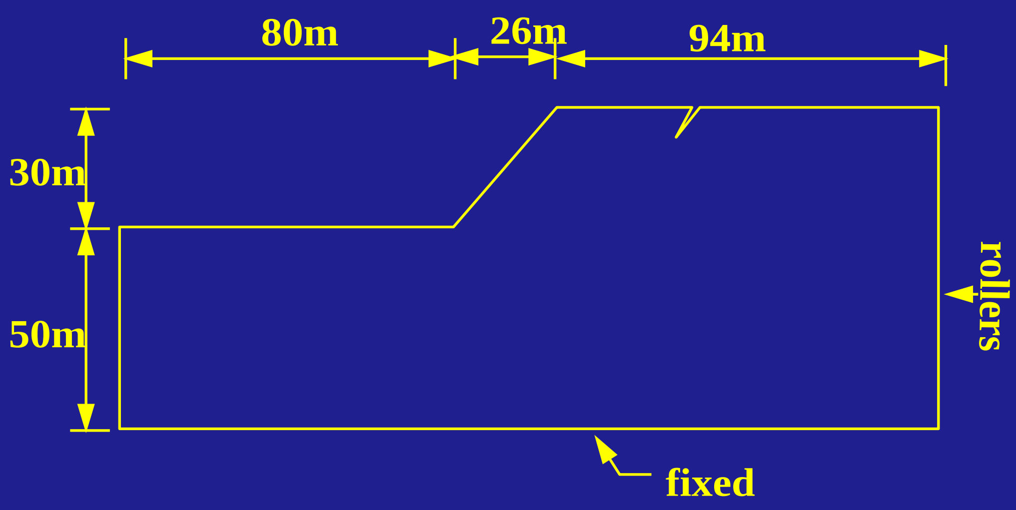

a) Undeformed slope.

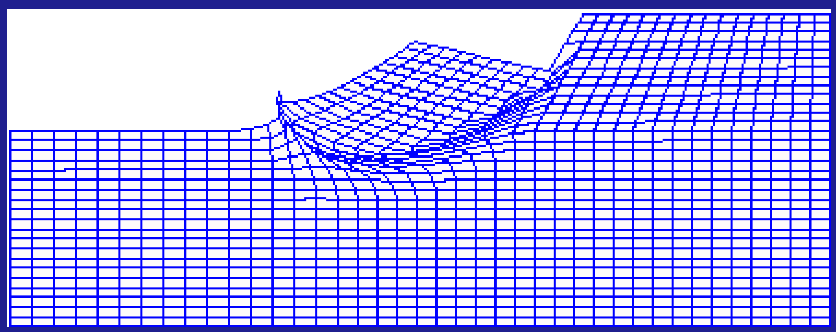

b) Deformed slope at limit state.

Steep Slope with tension crack 2

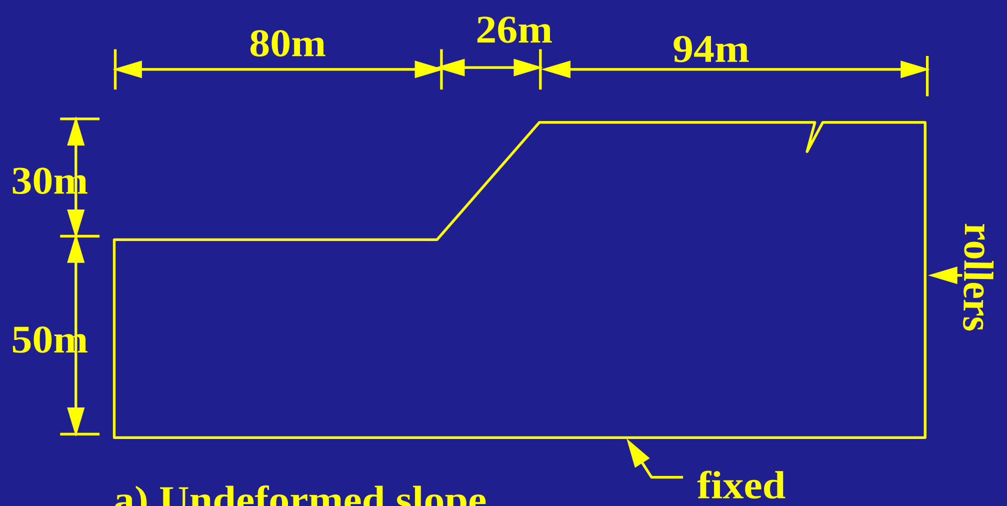

a) Undeformed slope.

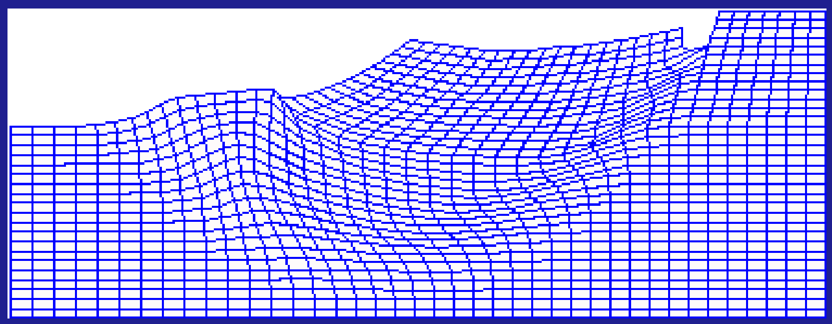

b) Deformed slope at limit state.

Slope with Building (Clay:α = 141kPa) : $(FS)_{grav}$=2.47

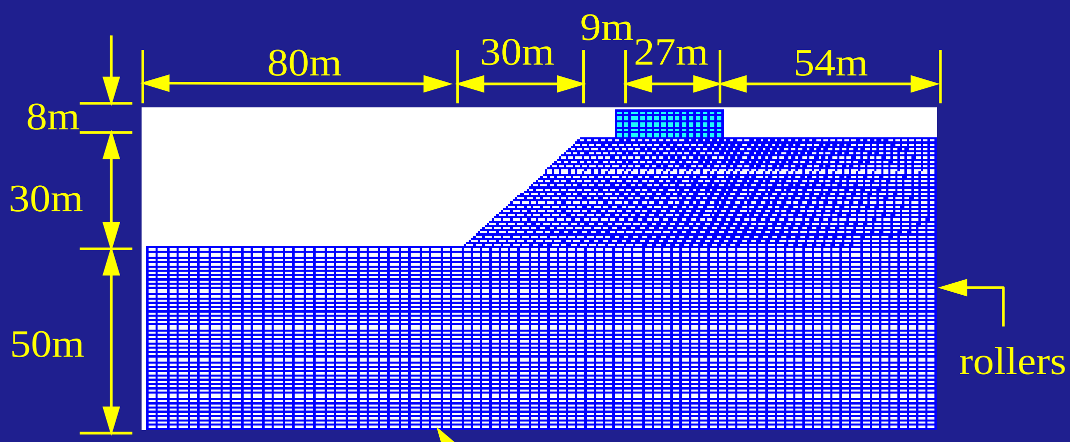

a)Undeformed state

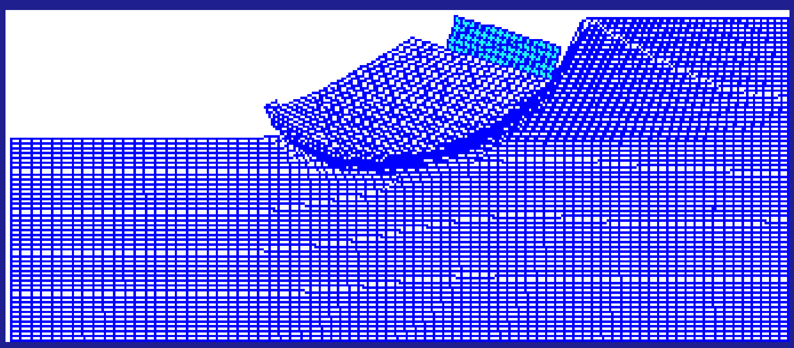

b)Deformed limit state

Slope under Pseudo−Static Earthquake Loading

g=9.81m/s^2 downward and leftward horizontal acceleration of 0.447g

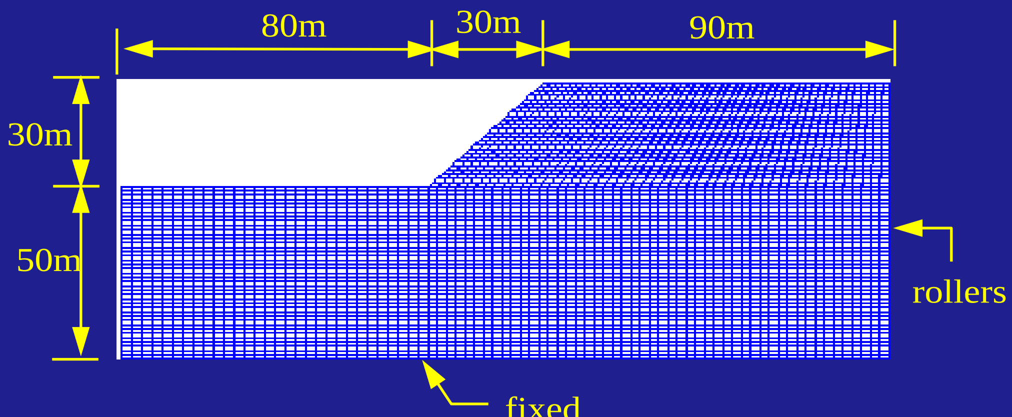

a)Undeformed Configuration

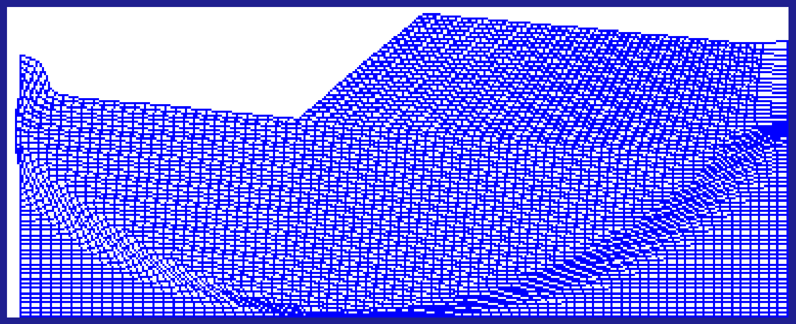

b)Deformed Configuration

Comparative Summary of the Two Continuum/FEM Approaches

1) Two methods employ virtually identical computational FEM techniques.

2) Computational times are competitive compared to classical methods of slice type.

3) In total stress analysis,neither method is clearly superior over the other

   * For purely cohesive soils, both methods yield identical results.

   * For frictional soils, strength reduction method typically gives more conservative results and it guarantees the existence of a limit state.

4) Gravity Increase Method :

   This method is well suited for analyzing the stability of embankment constructed on saturated soil deposits, since the rate of construction of embankment can be simulated with the rate at which gravity loading on the embankment is increased.

5) Strength Reduction Method:

   This method appears well suited for analyzing the stability of existing slopes in which unconfined active seepage is occurring

D.1 STABILITY ANALYSIS OF EMBANK−MENTS ON SATURATED DEPOSITS

A) Use a coupled porous medium model

* This model can capture the time dependent pore−pressure diffusion behaviors of a saturated porous medium.

B) Use the smooth elasto−plastic cap model

* This model can account for coupled shear and compressive soil behaviors.

C) Use the Gravity Increase Method

* This method can simulate the rate of embankment construction.

A. Continuum Formulation

Find $\mathbf{u}^s$ and $\mathbf{v}^w$, such that

$$\rho^s \mathbf{a}^s = \nabla \cdot \sigma' - n^s \nabla p_w - \xi \cdot (\mathbf{v}^s - \mathbf{v}^w) + \rho^s \mathbf{b}$$

$$\rho^w \frac{D^s}{Dt}(\mathbf{v}^w) = -n^w \nabla p^w + \xi \cdot (\mathbf{v}^s - \mathbf{v}^w) + \rho^w \mathbf{b}$$

Boundary Conditions

$\mathbf{u}^s = \bar{\mathbf{u}}^s$ on Γ_{gs}

$\mathbf{u}^w = \bar{\mathbf{u}}^w$ on Γ_{gw}

$(\sigma' - n^s p_w \delta)\mathbf{n} = \bar{\mathbf{h}}^s$ on Γ_{hs}

$-n^s p_w \mathbf{n} = \bar{\mathbf{h}}^w$ on Γ_{hw}

Initial Conditions

$\mathbf{u}^s(0) = \mathbf{u}_o{}^s$

$\dot{\mathbf{u}}^s(0) = \dot{\mathbf{u}}_o{}^s$

$\dot{\mathbf{u}}^w(0) = \dot{\mathbf{u}}_o{}^w$

Matrix Equations

$$\begin{bmatrix} \mathbf{M}^s & \mathbf{0} \\ \mathbf{0} & \mathbf{M}^w \end{bmatrix} \begin{bmatrix} \mathbf{a}^s \\ \mathbf{a}^w \end{bmatrix} + \begin{bmatrix} \mathbf{Z} & -\mathbf{Z} \\ -\mathbf{Z} & \mathbf{Z} \end{bmatrix} \begin{bmatrix} \mathbf{v}^s \\ \mathbf{v}^w \end{bmatrix} + \begin{bmatrix} n^s(\mathbf{d}^s, \mathbf{v}) \\ n^w(\mathbf{v}) \end{bmatrix} = \begin{bmatrix} \mathbf{f}^{s(ext)} \\ \mathbf{f}^{w(ext)} \end{bmatrix}$$

$$\mathbf{M}^\alpha = \int N_A \, \rho^\alpha \, N_B \, d\Omega$$

$$\mathbf{Z} = \int N_A \cdot \xi \cdot N_B \, d\Omega$$

$$\begin{bmatrix} n^s(\mathbf{d}^s, \mathbf{v}) \\ n^w(\mathbf{v}) \end{bmatrix} = \begin{bmatrix} \int B_A \, \sigma' \, d\Omega + \int N_A n^s \, p_W \, d\Omega \\ -\int \nabla N_A n^w \, p_W \, d\Omega \end{bmatrix}$$

$$\begin{bmatrix} \mathbf{f}^{s(ext)} \\ \mathbf{f}^{w(ext)} \end{bmatrix} = \begin{bmatrix} \int N_A \, \rho^s \, \mathbf{b} \, d\Omega + \int N_A \, \bar{\mathbf{h}}^s \, d\Gamma \\ \int N_A \, \rho^w \, \mathbf{b} \, d\Omega + \int N_A \, \bar{\mathbf{h}}^w \, d\Gamma \end{bmatrix}$$

Tangent operator

$$\begin{bmatrix} \mathbf{M}^s & \mathbf{0} \\ \mathbf{0} & \mathbf{M}^w \end{bmatrix} + \begin{bmatrix} \Delta t \gamma \mathbf{Z} & -\Delta t \gamma \mathbf{Z} \\ -\Delta t \gamma \mathbf{Z} & \Delta t \gamma \mathbf{Z} \end{bmatrix} + \begin{bmatrix} \Delta t^2 \beta (\mathbf{K} + \mathbf{C}^{ss}) & \Delta t^2 \beta \mathbf{C}^{sw} \\ \Delta t^2 \beta \mathbf{C}^{ws} & \Delta t^2 \beta \mathbf{C}^{ww} \end{bmatrix}$$

$$\mathbf{K} = \int B_A \, \mathbf{D} \, B_B \, d\Omega$$

$$\mathbf{C}^{\alpha\beta} = \int \lambda^w \, \frac{n^\alpha \, n^\beta}{n^w} \, \nabla N_A \, \nabla N_B \, d\Omega$$

B. Material Model Description

Sandler−DiMaggio Cap Model

Features:

* Five elasto−plastic subcases

* Singular tangent operators in the corner regions (no bulk stiffness)

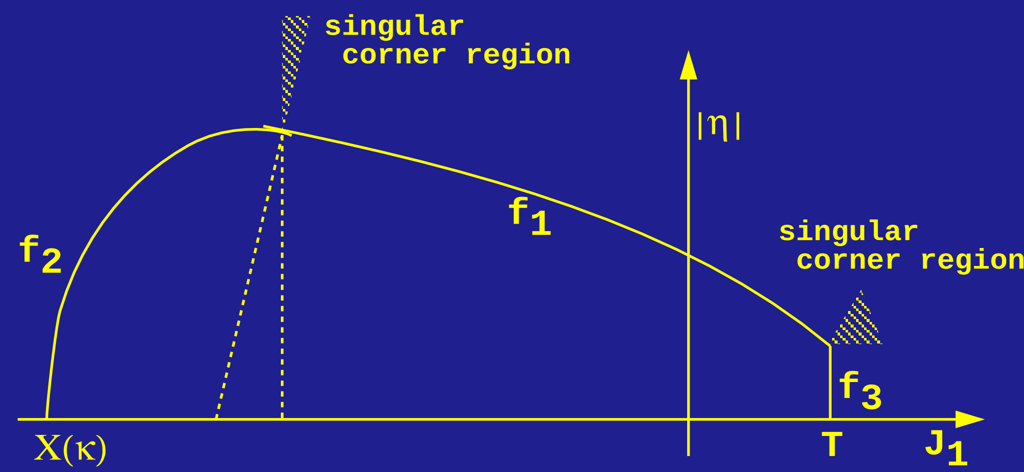

Smooth Cap Model

Features:

* Three elasto−plastic subcases

* No problems with singular tangent operators

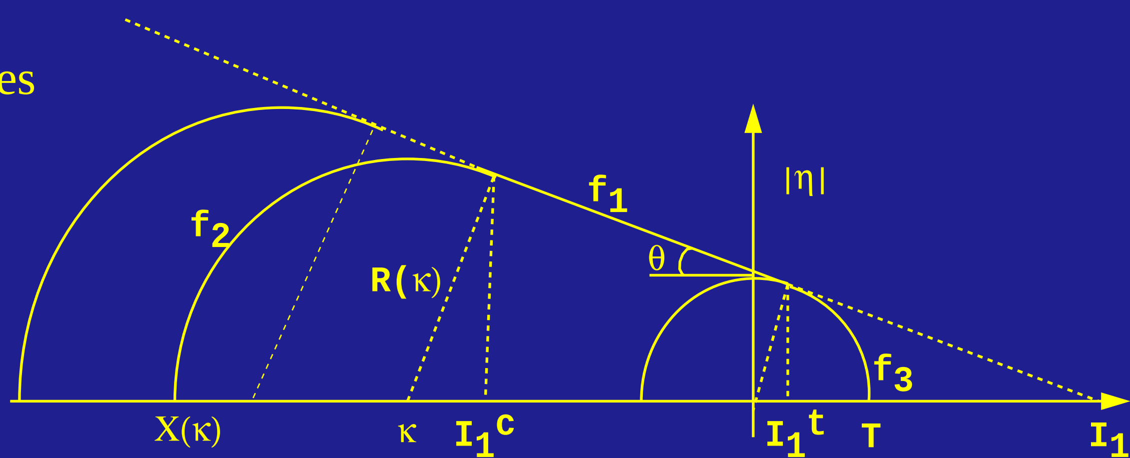

Yield functions

$$f_1(\sigma,\xi) = |\eta| - Fe(I_1) \leq 0 \qquad \text{where } F_e(I_1) = \alpha - \theta\, I_1$$

$$f_2(\sigma,\xi,\kappa) = |\eta|^2 - Fc(I_1,\kappa) \leq 0 \qquad \text{where } F_c(I_1,\kappa) = R^2(\kappa) - (I_1-\kappa)^2$$

$$f_3(\sigma,\xi) = |\eta|^2 - Ft(I_1) \leq 0 \qquad \text{where } F_t(I_1) = T^2 - I_1^{\,2}$$

Flow rule (associated)

$$\dot{\varepsilon}^p = \sum \gamma^\alpha \frac{\partial f_\alpha}{\partial \sigma}$$

Non−associated hardening laws

$$\dot{\mathbf{q}} = H\,\dot{\varepsilon}^p$$

$$\dot{\kappa} = h'(\kappa)\,tr(\dot{\varepsilon}^p) \quad \text{where } h'(\kappa) = \frac{\exp[-D\chi(\kappa)]}{WD\chi'(\kappa)} \;, \chi(\kappa) = \kappa - R(\kappa)$$

Karesh−Kuhn−Tucker Condition

$$f_\alpha \leq 0 \qquad \dot{\gamma}^\alpha \leq 0 \qquad \dot{\gamma}^\alpha f_\alpha = 0$$

Plastic consistency condition

$$\dot{\gamma}^\alpha \dot{f}_\alpha = 0$$

1−D Compression test on sand

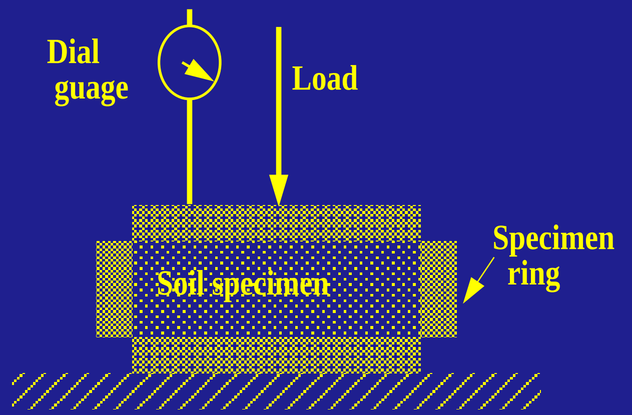

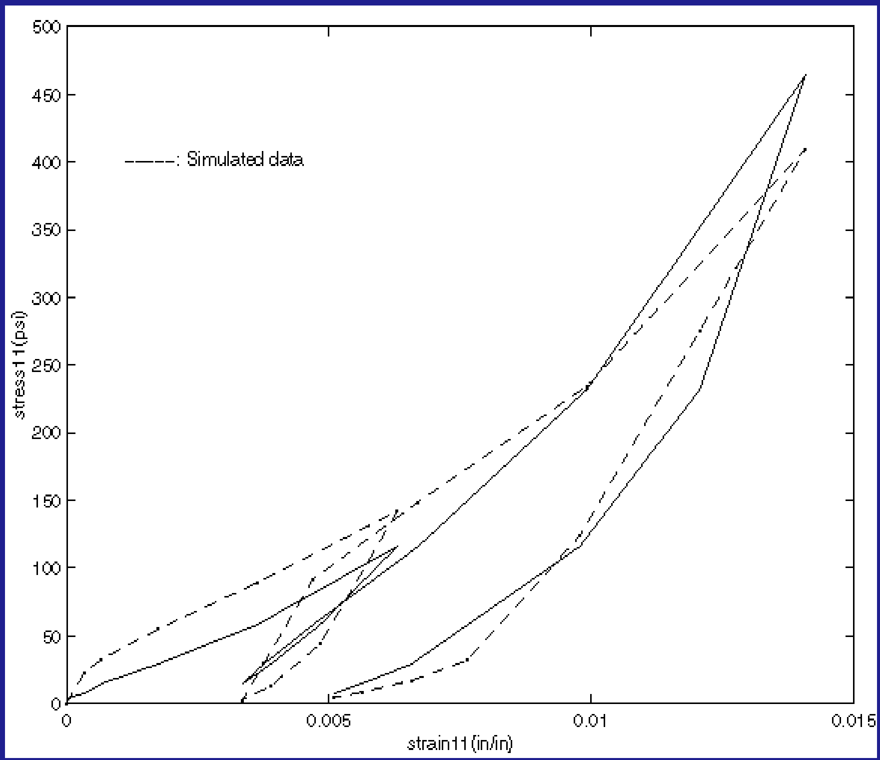

Experimental data and Model Response for 1−D compression on dry sand

Drained triaxial compression test

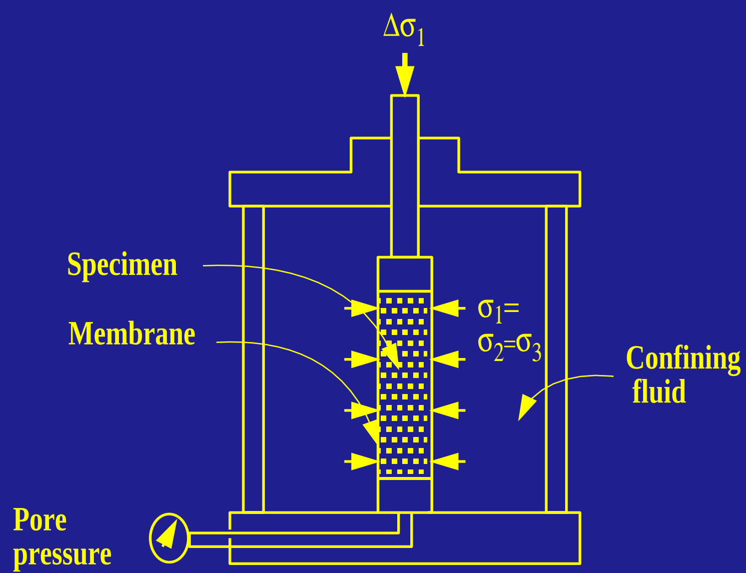

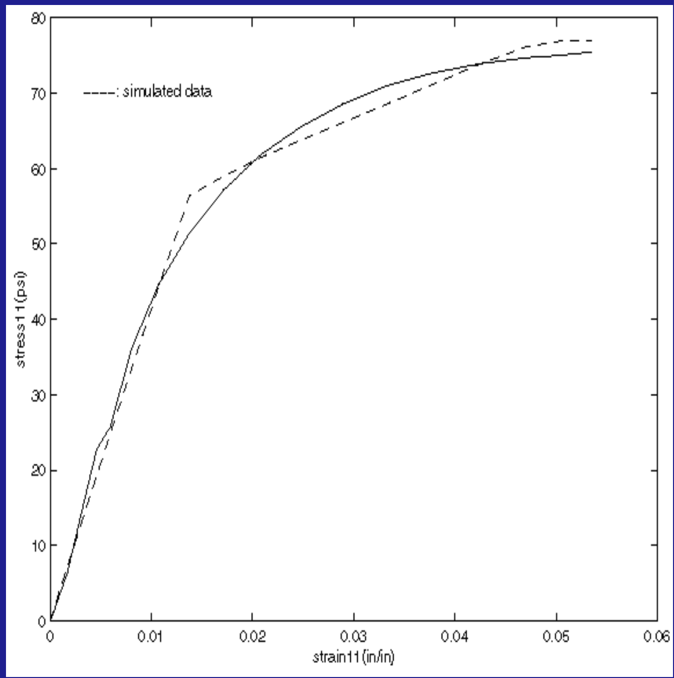

Experimental data and Model Response data for drained triaxial compression test

C. Examples

Cubzac –les–Point embankment in France

foundation: α=12.3kPa θ=0.2003, w=0.15, D=3.2e−7 Pa^{-1}

embankment: α=10.0Pa θ=0.2567, w=0.01, D=5.0e−7Pa^{-1}

* Experimental embankment constructed in 10 days up to failure in 1971.

* In 1982, Pilot et al anlalyzed the embankment's stability by Bishop's method of slices

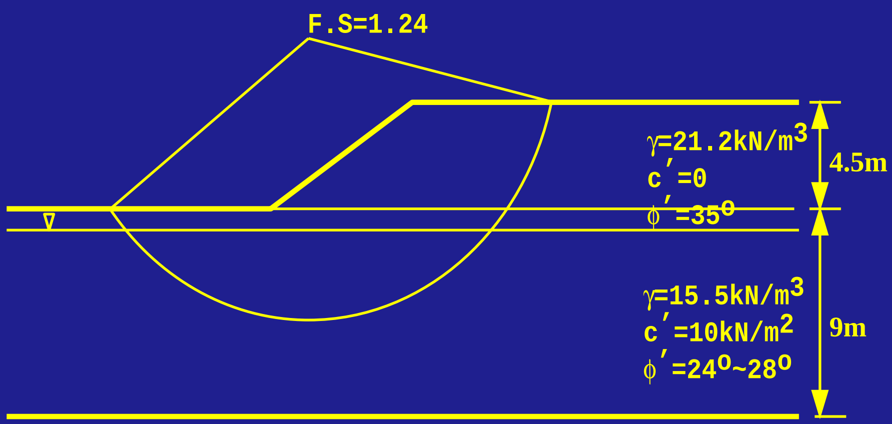

Mechanism and FS computed by Pilot

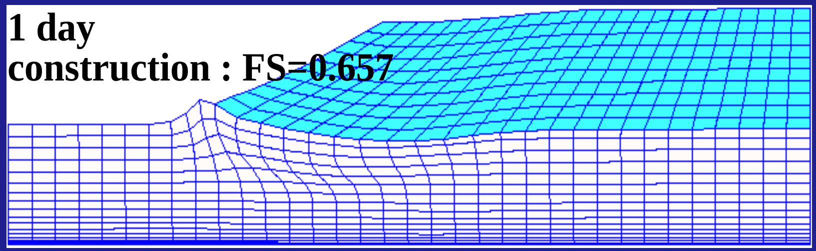

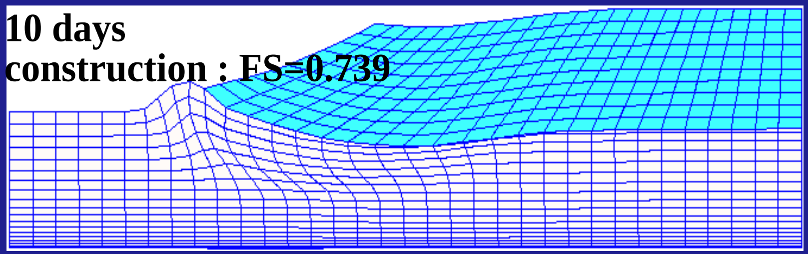

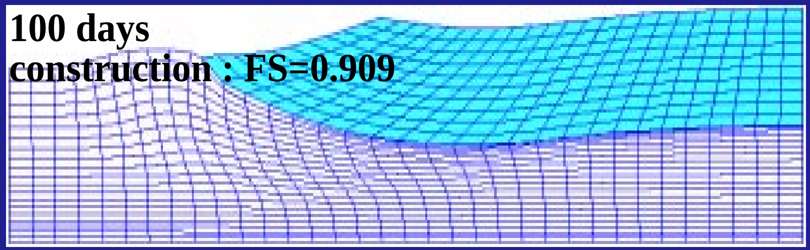

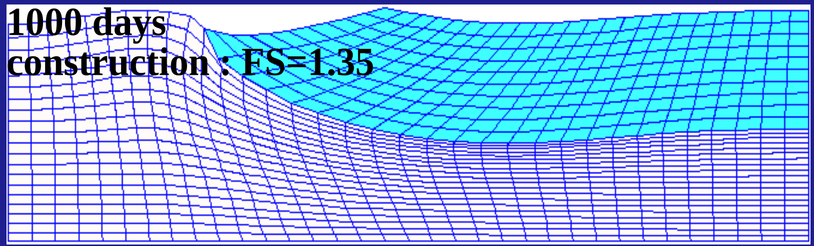

* Observation:

The computation method of SSA is more realistic (and conservative) than the classical method, since it accounts for the shear and compressibility behaviours of the clay soil.

Modeling of Sand Drains to Enhance Stability

without drains :FS=0.675

1 day construction : FS=0.968

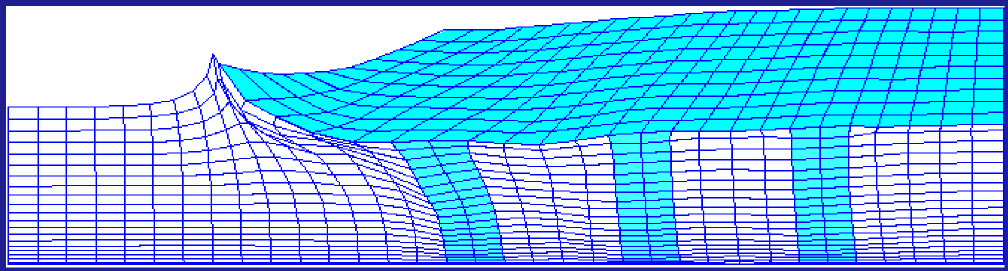

without drains :FS=0.739

10 days construction : FS=1.175

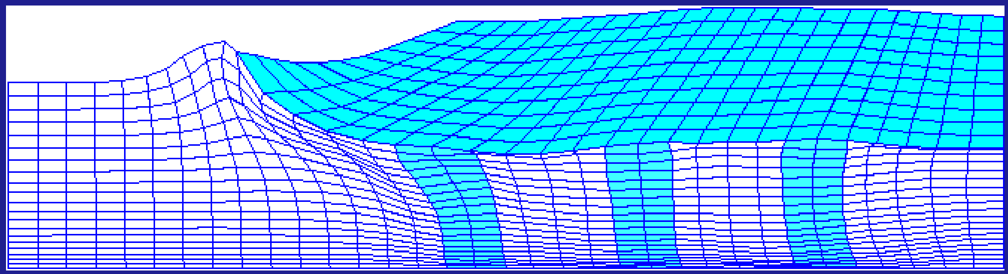

without drains :FS=0.909

100 days construction : FS=1.64

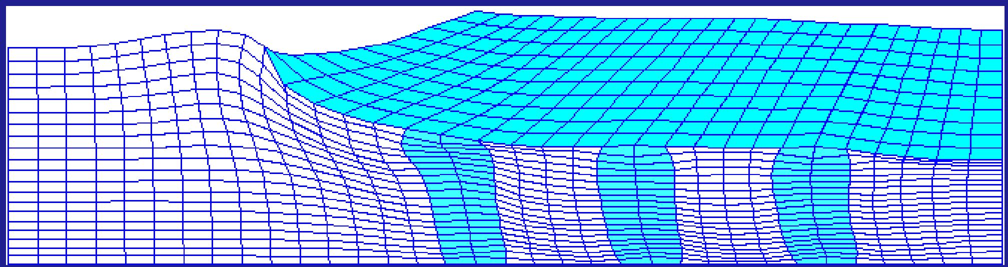

without drains :FS=1.35

1000 days construction : FS=2.61

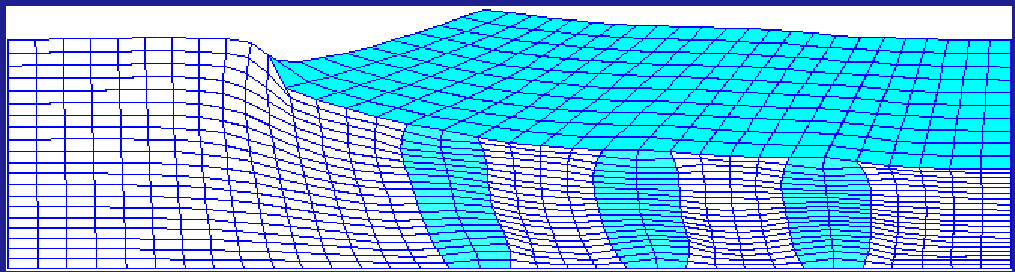

D.2 SLOPE STABILITY ANALYSIS WITH UNCONFINED SEEPAGE

A . Formulation

B. Example Solutions

A . Coupled Porous Medium Free−Boundary Problem

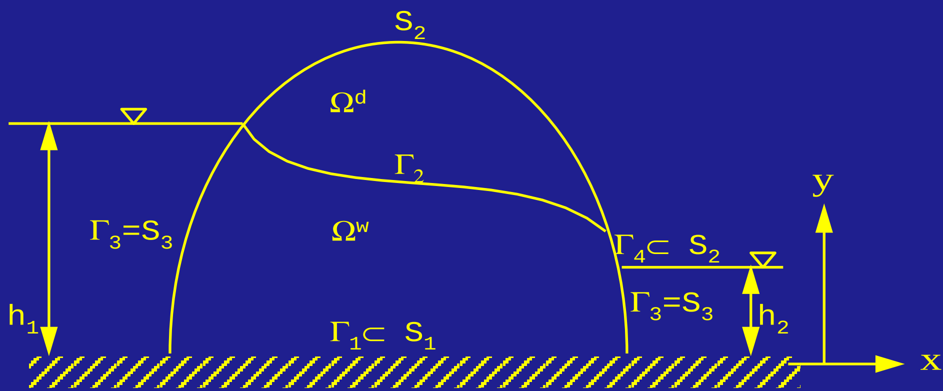

1) <u>Problem Geometry</u>

2) <u>Statement of the Problem</u>

Steady state seepage and incompressible fluid are assumed

Find $\mathbf{u}^s$ and p, such that

$$\nabla \cdot (\sigma' - p\delta) + \rho \mathbf{b} = 0 \quad \text{in } \Omega \quad \text{(Total Stress Equilibrium)}$$

$$\nabla \cdot \mathbf{v}^s + \nabla \cdot \mathbf{v}^w = 0 \quad \text{in } \Omega^w \quad \text{(Conservation of Fluid Mass)}$$

Solid Boundary Conditions

$$\mathbf{u}^s = \bar{\mathbf{u}}^s \quad \text{on } S_1$$

$$(\sigma' - p\delta) \cdot \mathbf{n} = \bar{\mathbf{h}}^s \quad \text{on } S_1 \cup S_2$$

Fluid Boundary Conditions

$$p > 0 \text{ in } \Omega^w \quad ; \; p=0 \text{ elsewhere}$$

$$\mathbf{n} \cdot \mathbf{v}^w = 0 \quad \text{on } \Gamma_1$$

$$p=0 \quad \text{and} \quad \mathbf{n} \cdot \mathbf{v}^w = 0 \quad \text{on } \Gamma_2$$

$$p = \bar{p} \quad \text{on } \Gamma_3$$

$$p=0 \quad \text{and} \quad -\mathbf{n} \cdot \mathbf{v}^w \leq 0 \quad \text{on } \Gamma_4$$

$$\text{where } \bar{p} = \begin{cases} \gamma_w (h_2 - y) \text{ on the right side of dam} \\ \gamma_w (h_1 - y) \text{ on the left side of dam} \end{cases}$$

$$\mathbf{v}^w = -\kappa \cdot \text{grad}\left(\frac{p}{\gamma_w} + y\right) \quad \text{(Darcy's Law)}$$

Purely Cohesiveless Soil

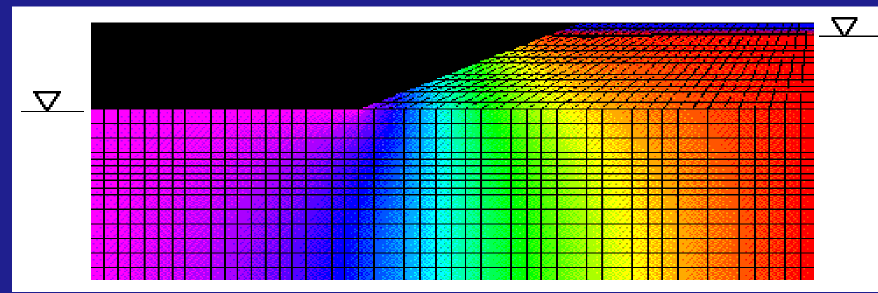

Strength Reduction Method (dry slopes)

Strength Reduction Method (seepage effects included)

H=6m (12%)

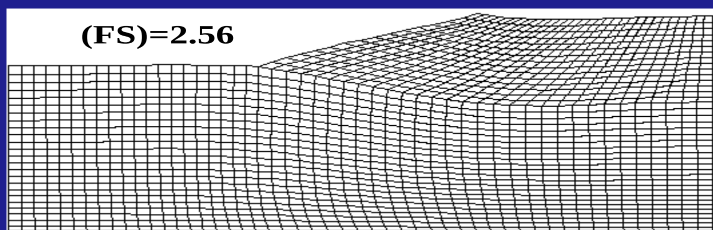

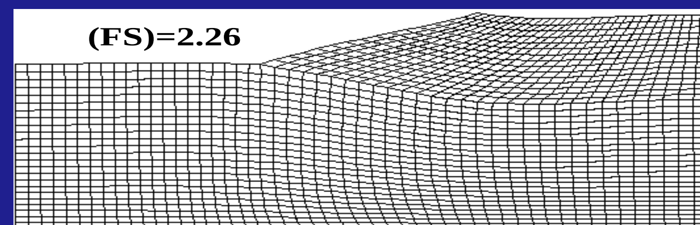

H=12m (14.7%)

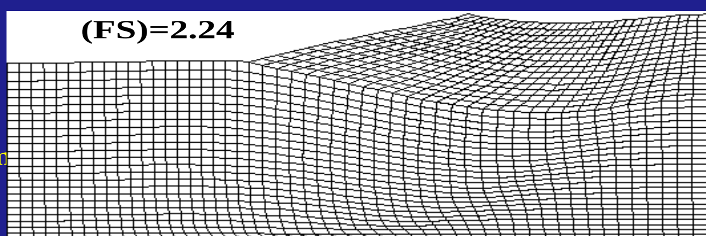

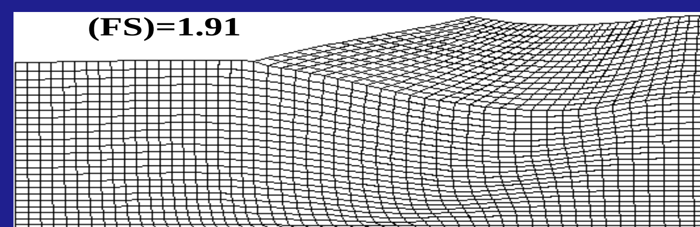

H=30m (18.5%)

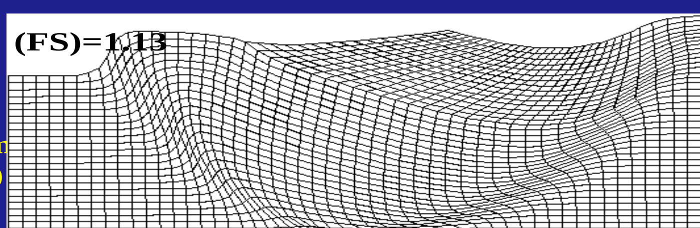

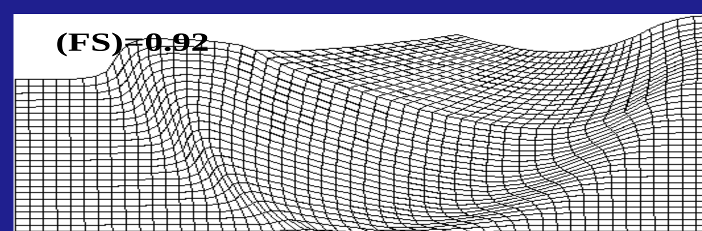

H=60m (19%)

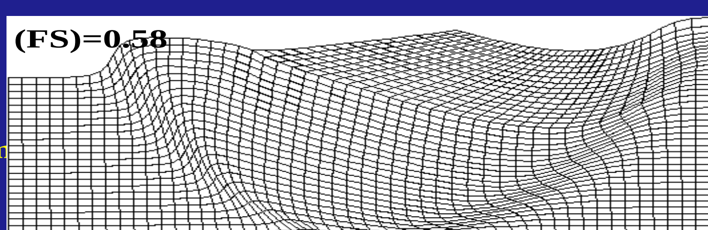

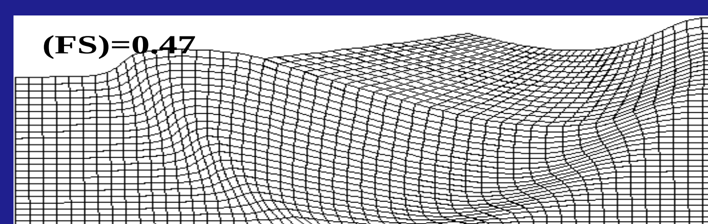

E. SUMMARY ON FEM SLOPE STABILITY ANALYSIS

1) Approximations required in SLICE type methods are not required.

2) The method can use virtually any realistic soil material model.

   * Usage of more sophisticated material models typically requires more laboratory testing.

3) For many applications, classical methods are suitable, given the uncertainty in soil properties.

4) FEM/SSA appears to hold an advantage over classical methods for problems involving seepage − as in embankment stability analysis.

5) Requirements for SSA with FEM are non−trivial.

* High−end PC or workstation
* FEM software (starting at $2k per year for commercial licenses)
* Understanding of soil mechanics, material models and FEM.

6) The 2D SSA examples presented here took between 15 minutes and a few hours to run on an engineering workstation (SGI Powerchallenge).

Presently, 3D SSA with FEM is too expensive to be feasible on PCs and workstations. In the future, this may become feasible as computing power advances.